



TITLE:

Dynamics of two key maternal factors that initiate zygotic regulatory programs in ascidian embryos

AUTHOR(S):

Oda-Ishii, Izumi; Abe, Tetsuya; Satou, Yutaka

CITATION:

Oda-Ishii, Izumi ...[et al]. Dynamics of two key maternal factors that initiate zygotic regulatory programs in ascidian embryos. *Developmental Biology* 2018, 437(1): 50-59

ISSUE DATE:

2018-05-01

URL:

<http://hdl.handle.net/2433/232532>

RIGHT:

© 2018. This manuscript version is made available under the CC-BY-NC-ND 4.0 license <http://creativecommons.org/licenses/by-nc-nd/4.0/>; The full-text file will be made open to the public on 1 May 2019 in accordance with publisher's 'Terms and Conditions for Self-Archiving'; This is not the published version. Please cite only the published version.; この論文は出版社版ではありません。引用の際には出版社版をご確認ください。

1 **Dynamics of two key maternal factors that initiate zygotic**
2 **regulatory programs in ascidian embryos**

3

4 Izumi Oda-Ishii, Tetsuya Abe, and Yutaka Satou

5 Department of Zoology, Graduate School of Science, Kyoto University, Kyoto 606-8502, Japan

6

7

8 Correspondence: Yutaka Satou, yutaka@ascidian.zool.kyoto-u.ac.jp

9

10

11 **Abstract**

12 In animal embryos, transcription is repressed for a definite period of time after fertilization. In the
13 embryo of the ascidian, *Ciona intestinalis* (type A; or *Ciona robusta*), transcription of regulatory genes is
14 repressed before the 8- or 16-cell stages. This initial transcriptional quiescence is important to enable the
15 establishment of initial differential gene expression patterns along the animal–vegetal axis by maternal
16 factors, because the third cell division separates the animal and vegetal hemispheres into distinct
17 blastomeres. Indeed, maternal transcription factors directly activate zygotic gene expression by the 16-
18 cell stage; Tcf7/ β -catenin activates genes in the vegetal hemisphere, and Gata.a activates genes in the
19 animal hemisphere. In the present study, we revealed the dynamics of Gata.a and β -catenin, and
20 expression profiles of their target genes precisely. β -catenin began to translocate into the nuclei at the 16-
21 cell stage, and thus expression of β -catenin targets began at the 16-cell stage. Although Gata.a is
22 abundantly present before the 8-cell stage, transcription of Gata.a targets was repressed at and before the
23 4-cell stage, and their expression began at the 8-cell stage. Transcription of the β -catenin targets may be
24 repressed by the same mechanism in early embryos, because β -catenin targets were not expressed in 4-
25 cell embryos treated with a GSK inhibitor, in which β -catenin translocated to the nuclei. Thus, these two
26 maternal factors have different dynamics, which establish the pre-pattern for zygotic genetic programs in
27 16-cell embryos.

28 **Keywords:** Ascidian; Zygotic gene activation; Gata; β -catenin

29 **Highlights**

- 30 ♦ The earliest transcription is detectable at the 8-cell stage in *Ciona* embryos
- 31 ♦ Gata.a is present in nuclei before initiation of expression of its targets

- 32 ♦ Nuclear translocation of β -catenin begins markedly at the 16-cell stage
- 33 ♦ Dynamics of Gata.a and β -catenin are regulated differently

34 1. Introduction

35 Maternal factors in animal embryos activate transcription from genomes of zygotes shortly
36 after fertilization, and subsequent developmental processes become dependent on zygotic transcripts
37 (Langley et al., 2014; Tadros and Lipshitz, 2009). This process is called the maternal-to-zygotic
38 transition, and the duration before transcription begins differs among different species.

39 *Ciona intestinalis* (type A), also known as *Ciona robusta*, is a tunicate, which belongs to the
40 sister group of vertebrates. In *Ciona* embryos, the first four cell divisions occur synchronously and the
41 cell cycle lengths are almost fixed (Dumollard et al., 2013; Hotta et al., 2007). Previous studies have
42 revealed that a small number of genes initiate expression after the fourth cell division (at the 16-cell
43 stage) by comprehensive expression assays (Imai et al., 2004; Matsuoka et al., 2013), although
44 expression of two transcription factor genes, *Foxa.a* and *Sox1/2/3*, begins at the 8-cell stage (Miya and
45 Nishida, 2003; Shimauchi et al., 2001). Maternal factors, including Gata.a and β -catenin, activate these
46 genes in three distinct partially overlapping domains at the 16-cell stage (Bertrand et al., 2003; Hudson
47 et al., 2013; Oda-Ishii et al., 2016; Rothbacher et al., 2007). Notably, *Foxd*, *Fgf9/16/20*, and *Tbx6b* are
48 activated by β -catenin in the vegetal hemisphere [*Tbx6.b* is also regulated by *Zic-r.a* (Macho-1) and
49 expressed only in the posterior vegetal cells]. *Efna.d* and *Tfap2-r.b* are activated by Gata.a in the animal
50 hemisphere, and Gata.a activity is suppressed through its interaction with β -catenin in the vegetal
51 hemisphere (Oda-Ishii et al., 2016). Since the animal and vegetal hemispheres do not segregate before
52 the 8-cell stage, the transcriptional quiescence before the 8-cell stage is important for establishing these

53 initial gene expression domains along the animal-vegetal axis. At subsequent stages, specific gene
54 expression patterns are established on the basis of this initial setup (Bertrand et al., 2003; Hudson et al.,
55 2013; Hudson et al., 2016; Imai et al., 2006; Satou and Imai, 2015). Why are these genes activated at the
56 8- and 16-cell stages, but not before these stages?

57 In the present study, we analyzed the following points to understand the regulatory
58 mechanisms of genes that are activated at the 16-cell stage: (1) when do the target genes of Gata.a and β -
59 catenin precisely initiate expression? Is the timing of beginning of their expression tightly controlled?
60 (2) When is β -catenin translocated into nuclei? (3) When and how much Gata.a is accumulated in nuclei
61 of early embryos?

2. Results

2.1. Zygotic transcription of regulatory genes begins weakly at the 8-cell stage and markedly increases by the 16-cell stage

Only two genes, *Sox1/2/3* (also known as *Soxb1*) and *Foxa.a*, have been identified to be expressed zygotically at the 8-cell stage (Miya and Nishida, 2003; Shimauchi et al., 2001). Furthermore, according to our previous studies that examined zygotic gene expression comprehensively (Imai et al., 2004; Matsuoka et al., 2013), only a small number of genes, including *Efna.d* and *Foxd*, are expressed at the 16-cell stage. We first confirmed by *in situ* hybridization that expression of *Foxa.a* and *Sox1/2/3* was not observed at or prior to the 4-cell stage (Fig. 1A and B), and that expression of *Efna.d*, *Tfap2-r.b*, *Foxd*, *Fgf9/16/20* and *Tbx6.b* was not observed at or prior to the 8-cell stage (Fig. 1C–G).

To examine the expression quantitatively, we analyzed the expression levels of *Foxa.a*, *Sox1/2/3*, *Efna.d*, *Tfap2-r.b*, *Foxd*, *Fgf9/16/20*, and *Tbx6.b* using reverse-transcription and quantitative PCR (RT-qPCR) in three independent experiments (Fig. 2A–G). The expression level of maternal *Gata.a* was also measured as a control (Fig. 2H). Consistent with the *in situ* hybridization results, *Foxa.a* mRNA was detected at the 8-cell stage. Although its expression level at the 8-cell stage was only 23% on average of that at the 16-cell stage, it was significantly higher than that at the 4-cell stage. Similarly, *Sox1/2/3* mRNA was detected at the 8-cell stage. In addition, although it was not detected by *in situ* hybridization, *Efna.d* mRNA was detected at the 8-cell stage using RT-qPCR. Similarly, *Tfap2-r.b*, which is also expressed in the animal hemisphere at the 16-cell stage (Imai et al., 2017; Imai et al., 2004) (Fig. 1D), was expressed weakly at the 8-cell stage. Although the expression levels of *Efna.d* and *Tfap2-r.b* at the 8-cell stage were 10% and 3% on average of those at the 16-cell stage, the differences between their

expression at the 4- and 8-cell stages were statistically significant. Thus, these results obtained from *in situ* hybridization and RT-qPCR indicated that *Foxa.a*, *Sox1/2/3*, *Efna.d*, and *Tfap2-r.b* begin to be expressed weakly at the 8-cell stage, and strongly at the 16-cell stage.

On the other hand, no significant increase in *Foxd* expression was detected between the 4- and 8-cell stages using RT-qPCR. The expression of *Fgf9/16/20*, which has the same pattern as *Foxd* expression at the 16-cell stage (Bertrand et al., 2003; Imai et al., 2002a) (Fig. 1F), and *Tbx6*, which is expressed only in the posterior vegetal cells (Takatori et al., 2004) (Fig. 1G), was not significantly different between the 4- and 8-cell stages. These observations suggested that *Foxd*, *Fgf9/16/20*, and *Tbx6.b* begin to be expressed strictly at the 16-cell stage.

A previous study reported that a construct containing 12 GATA-binding sites upstream of the *Brachyury* basal promoter was expressed at low levels at the 2-cell and 4-cell stages of *Ciona* embryos (Rothbächer et al., 2007). This result suggested that Gata.a might activate low level transcription of its targets in early embryos before the 8-cell stage. To test this possibility, we used a GFP reporter construct containing the upstream sequence of *Efna.d*, because the expression of the reporter gene was expected to be higher than that of endogenous *Efna.d*.

While this construct recapitulated the expression of endogenous *Efna.d* in 75% of the 16-cell embryos, we detected weak signals for the expression of *Efna.d* reporter in 23% of the 2-cell embryos (Fig. 3A). To quantify the amount of transcripts from the reporter construct, we examined the expression of the reporter construct by RT-qPCR (Fig. 3B). Expression level at the 8-cell stage was 11% on average of that at the 16-cell stage, which was consistent with the endogenous expression profile of *Efna.d* (see Fig. 2B). On the other hand, the expression levels at the 2- and 4-cell stages were considerably lower

than those at the 8- and 16-cell stages. Thus, although *Efna.d* may potentially be activated as early as the 2-cell stage, its expression was low and endogenous expression of *Efna.d* was rarely detected (see also Fig. 4C and the next section).

2.2. *Efna.d* transcription begins weakly in the vegetal cells and strongly in the animal cells

Expression of the reporter was stronger than that of endogenous *Efna.d*, and therefore, it was detected using *in situ* hybridization at the 8-cell stage (Fig. 4A). Similarly to the results of a previous study (Rothbächer et al., 2007), almost all embryos expressed the reporter strongly in the animal hemisphere, and almost a half of them also expressed the reporter in the vegetal hemisphere (Fig. 4B). However, expression in the vegetal cells was weak in most cases (Fig. 4B).

Next, to examine the expression of endogenous *Efna.d* in the animal and vegetal hemispheres, we prepared a set of intron primers that was designed to amplify a sequence within the first intron of *Efna.d*, in order to detect only its nascent transcripts. With this primer set, we rarely detected *Efna.d* transcripts in unfertilized eggs, fertilized eggs, 2-cell embryos, and 4-cell embryos (Fig. 4C), which was consistent with the observation in Figure 2C. This observation indicated that nascent transcripts of *Efna.d* could be detected with this method, even if a trace of maternal mRNA of *Efna.d* might be present. Next, we manually separated 8-cell embryos into the animal and vegetal halves using a glass needle, and analyzed them using RT-qPCR (Fig. 4D). While no amplification was detected in the negative control in which reverse transcriptase was not added, amplification was observed for cDNA pools derived from the animal halves and vegetal halves (Fig. 4E). However, the expression level of *Efna.d* was markedly lower in the vegetal halves than in the animal halves. Thus, although *Efna.d* expression began at the 8-cell stage and the expression was not limited to the animal hemisphere, it was higher in the animal

hemisphere than in the vegetal hemisphere.

2.3. Localization of Gata.a and β -catenin in the early embryo

Efna.d and *Tfap-2-r.b* are expressed in the animal hemisphere at the 16-cell stage under the direct control of Gata.a, while *Foxd*, *Fgf9/16/20*, and *Tbx6.b* are expressed in the vegetal hemisphere at the 16-cell stage under the direct control of Tcf7 and β -catenin (Hudson et al., 2013; Hudson et al., 2016; Imai et al., 2002b; Oda-Ishii et al., 2016; Rothbächer et al., 2007). Hence, we examined the distribution of Gata.a and β -catenin proteins.

We recently showed that Gata.a is distributed in all nuclei at the 16-cell stage (Oda-Ishii et al., 2016). Similarly, immunostaining signals for Gata.a were detected in the nuclei of the 2-, 4-, and 8-cell embryos (Fig. 5A). Western blots showed that the amount of Gata.a in unfertilized and fertilized eggs was approximately one-half to two-thirds of that at the 16-cell stage, and that a maximum level was reached as early as the 4-cell stage (Fig. 5B). This observation suggested that suppression of *Efna.d* and *Tfap2-r.b* expression at the 4-cell stage or earlier is not due to the limited supply of Gata.a.

As reported previously (Hudson et al., 2013), at the 16-cell stage, β -catenin was detected in the nuclei of cells in the vegetal hemisphere but not in those in the animal hemisphere (Fig. 5C). No clear nuclear signal was detected between the 2- to 8-cell stages (Fig. 5C). This was consistent with the observation that *Foxd*, *Fgf9/16/20*, and *Tbx6.b* were not expressed before the 16-cell stage (Fig. 1 and Fig. 2).

Next, we compared the intensity of signals between nuclei and cytoplasm. Because β -catenin was not detected uniformly within the cytoplasm and detected strongly around the nuclei, we selected

areas with strong signals within the cytoplasm for comparisons with nuclear signals. At the 16-cell stage, nuclear signal for β -catenin was markedly stronger in the vegetal cells than in the animal cells (Fig. 5D). In addition, nuclear signal of β -catenin was slightly, but significantly, higher in the vegetal cells than in the animal cells of 8-cell embryos, although nuclear signals were less evident by immunostaining (Fig. 5C). Namely, our observation indicated that a small amount of β -catenin begin to be translocated into the nuclei of the vegetal cells at the 8-cell stage, and more β -catenin is translocated into the nuclei of the vegetal cells at the 16-cell stage. The initial small difference between the animal and vegetal hemispheres at the 8-cell stage may explain why *Efna.d* was expressed more strongly in the animal hemisphere than in the vegetal hemisphere of the 8-cell embryo, because β -catenin suppresses the activity of Gata.a (Oda-Ishii et al., 2016; Rothbacher et al., 2007) (see Discussion).

2.4. *Pem-1* is not responsible for transcriptional quiescence in early embryos

Pem-1 is localized in the posterior-most cells, which contribute to germ line cells, and suppresses transcription in the germ line (Kumano et al., 2011; Shirae-Kurabayashi et al., 2011; Yoshida et al., 1996). It has been reported that, in *Pem-1* morphants, in which a specific morpholino antisense oligonucleotide (MO) against *Pem1* was injected, *Foxa.a* was expressed not only in the anterior cells but also in the posterior cells at the 8-cell stage (Shirae-Kurabayashi et al., 2011). It has also been reported that, in another ascidian, *Halocynthia roretzi*, the expression of several genes, including *Noto* (*Not*), were detectable at the 4-cell stage, and *Noto* expression was detected in some *Pem-1* morphants at the 2-cell stage (Kumano et al., 2011). These reports motivated us to examine *Foxd* and *Efna.d* expression in *Pem-1* morphants. As reported previously (Kumano et al., 2011; Shirae-Kurabayashi et al., 2011), *Foxa.a* was expressed ectopically in the posterior blastomeres (Fig. 6A), suggesting that *Pem-1* was successfully

knocked down by our MO, which was different from the MOs used in the previous study (Shirae-Kurabayashi et al., 2011). On the other hand, *Efna.d* and *Foxd* were not precociously expressed at the 8-cell stage (Fig. 6B and C). Note that our observation does not mean that these two genes are not regulated by Pem-1 (see Fig 7E). However, it indicates that transcriptional silence in early *Ciona* embryos is not explained by Pem-1 function only.

2.5. Nuclear β -catenin can activate its target after the third cell division but not after the second division

Nuclear β -catenin is required for *Foxd* expression (Hudson et al., 2013; Hudson et al., 2016; Imai et al., 2002b; Oda-Ishii et al., 2016) and was first observed in vegetal cells at the 16-cell stage as we showed in Fig. 5C. Therefore we reasoned that regulation of nuclear translocation of β -catenin was the key to determine the timing of *Foxd* expression. To examine this hypothesis, we treated embryos with BIO, a specific inhibitor for Gsk3. This treatment stabilizes β -catenin and leads to the ectopic activation of genes downstream of β -catenin (Hudson et al., 2013). In BIO-treated embryos, β -catenin was detected prematurely in the nuclei at the 4- and 8-cell stages (Fig. 7A and B). While the relative fluorescence intensity (nuclei to cytoplasm) was 0.30 in normal untreated 4-cell embryos (see Fig. 5D), it was increased to 0.95 in the BIO-treated 4-cell embryos and to similar levels in the animal and vegetal cells of BIO-treated 8-cell embryos (Fig. 7C). In BIO-treated embryos, *Foxd* expression was detected at the 8-cell stage using RT-qPCR (Fig. 7D) and *in situ* hybridization (Fig. 7E). Note that we did not detect *Foxd* expression in the most posterior vegetal cells, in which Pem-1 is localized, of these experimental embryos. On the other hand, *Foxd* expression level was low at the 4-cell stage (Fig. 7D). Thus, *Foxd* was rarely activated at the 4-cell stage, even if its activator was present.

187 The above result showed that *Foxd* could be activated at the 8-cell stage, if β -catenin was
188 present. Therefore, we further confirmed that the fourth cell division between the 8- and 16-cell stages
189 was not required for this activation with the following experiment. We injected a MO against *Cdc25*,
190 because *Cdc25* is a phosphatase that promotes the transition from the G2 phase to the M phase, and this
191 protein has a similar function in *Ciona* embryos (Ogura et al., 2011; Ogura and Sasakura, 2016). While
192 injection of the control *lacZ* MO did not affect cell cycle lengths, injection of the *Cdc25* MO increased
193 cell cycle lengths (Fig. 8A). Approximately 110 min after fertilization, control embryos were at the 8-
194 cell stage, whereas *Cdc25* morphants were at the 4-cell stage. Approximately 130 min after fertilization,
195 control embryos were at the 16-cell stage, whereas the *Cdc25* morphants were at the 8-cell stage (Fig.
196 8B).

197 While *Foxd* normally begins to be expressed at the 16-cell stage (Imai et al., 2002b) (see Fig.
198 1E and Fig. 2E), *Foxd* expression was detected in 69% of *Cdc25* morphants at the 8-cell stage (130 min
199 after fertilization) but not at the 4-cell stage (110 min after fertilization) (Fig. 8C and D). Note that *Foxd*
200 was not expressed in the posterior vegetal cells (B4.1) probably because of transcriptional suppression
201 by Pem-1. The expression level of *Foxd* in *Cdc25* morphants was 11 % on average of that in normal
202 embryos at 130 min after fertilization (Fig. 8E). However, this does not necessarily mean that
203 transcription of *Foxd* in *Cdc25* morphants was weaker than that in normal or *lacZ*-MO injected embryos
204 at 130 min after fertilization. First, *Foxd* was expressed in only one pair of cells in 69% of *Cdc25*
205 morphants, while it was expressed in three pairs of cells in all embryos injected with the *lacZ* MO.
206 Second, the time duration for which *Foxd* was expressed might also have been different between these
207 two experimental conditions. Even if so, the above result indicated that the fourth cell division was not
208 required for activating *Foxd*, and availability of its activator was important for determining timing of

209 *Foxd* expression.

3. Discussion

The target genes of Gata.a and β -catenin examined in the present study began to be expressed at the 8- and 16-cell stages, respectively. Consistently, the dynamics of Gata.a and β -catenin were regulated differently. Namely, Gata.a was present abundantly in unfertilized eggs, and was also produced rapidly after fertilization, while nuclear translocation of β -catenin began at the 8-cell stage and markedly increased in the vegetal cells at the 16-cell stage. In addition, transcription of the β -catenin and Gata.a targets was repressed at and before the 4-cell stage. Our data indicates that this repression and the dynamics of Gata.a and β -catenin determine the timing of zygotic transcription of the β -catenin and Gata.a targets in ascidian embryos.

The number of cell cycles is known to be important for determining the timing of zygotic genome activation (ZGA). In amphibians, the ratio of nucleus to cytoplasm is important for the ZGA, and this ratio increases rapidly following cell divisions (Kobayakawa and Kubota, 1981; Newport and Kirschner, 1982a, b). In *Drosophila* embryos, however, the timing of zygotic transcription for a majority of genes is determined by the absolute time or developmental stage, whereas the timing of zygotic transcription for a subset of genes is also determined by the nucleocytoplasmic ratio or cell cycle number (Lu et al., 2009). In *Caenorhabditis elegans*, maternal factors sequestering TAF-4, a basic transcription factor, in the cytoplasm are degraded prior to ZGA (Güven-Ozkan et al., 2008). In addition, rapid cell cycles prevent efficient transcription, because the inhibition of cell cycles before ZGA prematurely initiates transcription (Edgar and Schubiger, 1986; Kimelman et al., 1987). These mechanisms may work in concert to determine the timing of ZGA (Langley et al., 2014). Such global mechanisms may or may not be involved in determining the timing of expression of the β -catenin and Gata.a targets, as discussed below.

232 The observation that *Foxd* was expressed in 8-cell embryos treated with BIO indicated that β -
233 catenin targets had the potential to be activated at the 8-cell stage and nuclear translocation of β -catenin
234 was the key for initiation of their expression. Because *Foxd* was also expressed in *Cdc25* morphants at
235 the 8-cell stage, the number of cell divisions or cell cycles is not likely to be the determinant for
236 initiation of *Foxd* expression. Instead, the absolute time after fertilization may be important for this
237 regulation. Because *Foxd* was precociously expressed in BIO-treated embryos, negative regulators for
238 nuclear translocation of β -catenin may play a critical role in this process. Five novel maternal genes that
239 might regulate the nuclear localization of β -catenin have been identified in *Ciona* embryos (Wada et al.,
240 2008). These gene products may act as negative regulators for nuclear translocation of β -catenin.

241 Meanwhile *Foxd* was not precociously expressed in 4-cell embryos treated with BIO.
242 Similarly, the Gata.a targets were rarely expressed at the 4-cell stage, although Gata.a was present almost
243 at the same level in 4- or 8-cell embryos as in 16-cell embryos. In addition, *Foxa.a*, which is clearly
244 expressed at the 8-cell stage, was not expressed at the 4-cell stage or earlier. These observations
245 consistently indicated that low transcriptional activity was maintained at the 4-cell stage or earlier by
246 another mechanism, for which the number of cell divisions or cell cycles may be important. The reporter
247 construct that contained the upstream sequence of *Efna.d* was activated weakly at the 2- or 4-cell stage.
248 It is possible that the epigenetic state of the reporter was different from that of the genomic DNA in early
249 embryos and so the reporter was more competent to transcription. Even if so, our results indicated that
250 even exogenous DNAs were not effectively activated at the 2- or 4-cell stage, and simultaneously that
251 this mechanism may not be able to suppress transcription completely. The observation that *Efna.d* was
252 not transcribed at the 8-cell stage as strongly as at the 16-cell stage indicated that transcription
253 suppression gradually declines. This mechanism might globally repress transcription in early embryos.

254 A previous study indicated that Pem-1 prevents the nuclear accumulation of β -catenin in the
255 posterior-most cells (B5.2) of *Halocynthia* embryos (Kumano and Nishida, 2009). Because this function
256 of Pem-1 is restricted to the posterior-most cells, it is unlikely that Pem-1 controls the timing of β -
257 catenin nuclear localization in the entire embryo. We also observed nuclear accumulation of β -catenin in
258 the posterior-most cells of *Ciona* embryos. Therefore, it is not likely that Pem-1 prevents β -catenin
259 nuclear accumulation in *Ciona* embryos.

260 Pem-1 is also suggested to suppress transcription in the germ line by interacting with pTEF-1
261 and/or Groucho (Kumano et al., 2011; Shirae-Kurabayashi et al., 2011). Namely, loss of Pem-1 activity
262 is required for transcription, and therefore this maternal protein is related to the timing of transcriptional
263 initiation. However, because *Efna.d* and *Foxd* were not detected precociously in *Pem-1* morphants at the
264 8-cell stage by in situ hybridization, transcriptional suppression by Pem-1 cannot alone explain the
265 timing of transcriptional initiation in *Ciona* embryos.

266 In the present study, we analyzed the expression of genes for transcription factors and
267 signaling molecules only. However, it is likely that transcription of other non-regulatory genes is also
268 repressed before the 8-cell stage with the following two reasons. First, previous studies have failed to
269 find genes zygotically expressed before the 8-cell stage in *Ciona* embryos (Fujiwara et al., 2002;
270 Matsuoka et al., 2013; Nishikata et al., 2001). Second, the second serine residue of the C-terminal
271 domain (CTD) repeats of RNA polymerase II is not phosphorylated before the 8-cell stage, which
272 indicates transcriptional elongation (Shirae-Kurabayashi et al., 2011). Although we cannot completely
273 rule out a possibility that low level transcription occurs in early embryos, it is possible that a common
274 mechanism represses transcription of regulatory and non-regulatory genes in early embryos.

4. Conclusions

Most regulatory genes that begin to be expressed at the 16-cell stage are activated under the control of either β -catenin or Gata.a, and Gata.a activity is controlled by nuclear β -catenin (Bertrand et al., 2003; Imai et al., 2000; Oda-Ishii et al., 2016; Rothbächer et al., 2007). These Gata.a and β -catenin targets are required for activating their downstream genes in the animal and vegetal hemispheres, respectively (Bertrand et al., 2003; Hudson et al., 2016; Imai et al., 2017; Imai et al., 2016; Imai et al., 2006; Imai et al., 2002b; Ohta and Satou, 2013; Ohta et al., 2015). Nevertheless, *Efna.d* was expressed weakly in the vegetal hemisphere of 8-cell embryos, probably because nuclear translocation of β -catenin was considerably less and insufficient for complete suppression of Gata.a activity in the vegetal hemisphere of 8-cell embryos. This observation suggested that low expression of Gata.a targets in the vegetal hemisphere is not sufficient for activating their downstream pathways and therefore it is not harmful.

Our study indicated that dynamics of β -catenin and Gata.a, which are essential for the initiation of transcription of regulatory genes, are regulated differently in *Ciona* embryos. These dynamics prevent genes from being activated strongly before the animal and vegetal hemispheres are separated into distinct blastomeres, and establish the pre-pattern for zygotic genetic programs in 16-cell embryos.

5. Materials and Methods

5.1. Animals and cDNAs

295 *C. intestinalis* (type A; also called *C. robusta*) adults were obtained from the National Bio-
296 Resource Project for *Ciona intestinalis*. The cDNA clones were obtained from our EST clone collection
297 (Satou et al., 2005). Identifiers for genes examined in the present study are shown in Table 1.

298 **5.2. Morpholino antisense oligonucleotides and reporter constructs**

299 The MO (Gene Tools, LLC) against *Cdc25*, which blocked translation of *Cdc25* mRNA, was
300 used for the knockdown experiments (5'- GGAGTCCGTCATATTAAAGACAGGT-3'). The MO was
301 introduced by microinjection under a microscope. Because *Cdc25* encodes a phosphatase that promotes
302 cell cycles, slower cell cycles were expected in *Cdc25* morphants, and the expected phenotype was
303 obtained. The sequence of the MO against *Pem-1* was 5'-AAATACTGTGCATGTTTACATTCAT-3'. The
304 expression pattern of *Foxa.a* in embryos injected with this MO was the same as that in embryos injected
305 with a *Pem-1* MO that has been used in a previous study (Shirae-Kurabayashi et al., 2011).

306 The upstream sequence used for constructing the reporter construct for *Efna.d* was from
307 KhC3: 2,806,730–2,810,100 of the KH version of the genome sequence of *Ciona* (Satou et al., 2008).
308 The reporter construct was introduced by electroporation.

309 **5.3. Whole-mount *in situ* hybridization and RT-qPCR**

310 *In situ* hybridization was performed as described previously (Satou et al., 1995). For
311 quantifying endogenous gene expression by RT-qPCR (except for the experiment in Figure 4C and E),
312 we used the Cell-to-Ct kit (Thermo-Fisher Scientific). For each measurement, 50 embryos were lysed.
313 Each specimen was divided into two fractions. Reverse transcriptase was added to one fraction, and
314 water into the other fraction [the RT(-) control]. No amplification was observed in the RT(-) controls.

Because *Zic-r.a* is a maternal mRNA (Nishida and Sawada, 2001; Satou et al., 2002), and its amount is thought to remain constant in the early embryos, we used it as an internal control. Taqman chemistry was used for qPCR. The probes and primers are listed in Table 2.

For quantifying endogenous *Efna.d* expression using RT-qPCR in the experiment shown in Figure 4C and E, RNA was extracted using the RNeasy kit (Qiagen) from isolated blastomeres. In Figure 4C, 50 eggs/embryos were used for each of three independent experiments. In Figure 4E, 74 and 100 partial embryos were used for the first and second independent experiments, respectively. After DNase treatment, each specimen was divided into two fractions. One was used for setting up the RT(-) controls, in which no amplification was observed. In this experiment, we used a primer set that are designed to amplify a region within the first intron of *Efna.d* to detect the nascent transcripts (Table 2). SYBR Green chemistry was used for qPCR. Specific amplifications were confirmed by melting curve analyses. *Pou2* was used as the internal control, because *Pou2* mRNA is maternally expressed and not localized in specific blastomeres.

For measuring the expression of the reporter gene, *Efna.d>Gfp*, 100 embryos were collected, and RNA was extracted from them using the RNeasy kit (Qiagen). After DNase treatment, each specimen was divided into two fractions. Reverse transcriptase was added to one fraction and water into the other fraction. We detected amplification in the RT(-) controls, probably because a large amount of the reporter DNA was introduced and therefore it was not completely removed by the DNase treatment. We calculated the amount of RNA-derived cDNA by comparison between each pair of RT(+) and RT(-) samples. SYBR Green chemistry was used for qPCR. Specific amplifications were confirmed by melting curve analyses.

5.4. Western blotting and immunostaining

Antibodies against Gata.a and Tcf7 were made in our previous study (Oda-Ishii et al., 2016). An antibody against β -catenin was produced in a previous study (Kawai et al., 2007), and was a kind gift from Professor Hiroki Nishida of Osaka University, Japan. For western blotting, 200 embryos were lysed and loaded into each lane. Bands were quantified as arbitrary units by an imager (ChemiDoc XRS, BioRad) using Quantity-One software (BioRad). To detect protein localization, embryos were fixed with 3.7% formaldehyde in PBS for detection of Gata.a and with 1% paraformaldehyde in sea water for detection of β -catenin. The TSA plus kit (Perkin Elmer) was used for fluorescence detection.

ImageJ was used for quantification of fluorescence intensities. For each cell, a section with clear DAPI signal was chosen, and fluorescence intensity in a circle with a diameter of 20 pixels within the nucleus was quantified. Next, from the same slice, we chose the same size of cytoplasmic region that was strongly stained with the anti- β -catenin antibody, and quantified fluorescent intensity.

348 **Acknowledgements**

349 We thank Dr. Reiko Yoshida, Dr. Satoe Aratake, Dr. Manabu Yoshida and other members
350 working under the National Bio-resource project (MEXT, Japan) for providing experimental animals.
351 We also thank Professor Hiroki Nishida for providing us with the anti- β -catenin antibody.

352 **Funding**

353 This study was supported by Grants-in-aid from the Japan Society for the Promotion of
354 Science (grant numbers 15K14447, 17KT0020) and a grant from Sumitomo Foundation (140235 to YS).
355 This study was also supported partly by the CREST program of the Japan Science and Technology
356 Agency (JPMJCR13W6).

357

References

- Bertrand, V., Hudson, C., Caillol, D., Popovici, C., Lemaire, P., 2003. Neural tissue in ascidian embryos is induced by FGF9/16/20, acting via a combination of maternal GATA and Ets transcription factors. *Cell* 115, 615-627.
- Dumollard, R., Hebras, C., Besnardeau, L., McDougall, A., 2013. Beta-catenin patterns the cell cycle during maternal-to-zygotic transition in urochordate embryos. *Dev Biol* 384, 331-342.
- Edgar, B.A., Schubiger, G., 1986. Parameters Controlling Transcriptional Activation during Early *Drosophila* Development. *Cell* 44, 871-877.
- Fujiwara, S., Maeda, Y., Shin-I, T., Kohara, Y., Takatori, N., Satou, Y., Satoh, N., 2002. Gene expression profiles in *Ciona intestinalis* cleavage-stage embryos. *Mech Dev* 112, 115-127.
- Güven-Ozkan, T., Nishi, Y., Robertson, S.M., Lin, R.L., 2008. Global transcriptional repression in *C. elegans* germline precursors by regulated sequestration of TAF-4. *Cell* 135, 149-160.
- Hotta, K., Mitsuhashi, K., Takahashi, H., Inaba, K., Oka, K., Gojobori, T., Ikeo, K., 2007. A web-based interactive developmental table for the ascidian *Ciona intestinalis*, including 3D real-image embryo reconstructions: I. From fertilized egg to hatching larva. *Dev Dyn* 236, 1790-1805.
- Hudson, C., Kawai, N., Negishi, T., Yasuo, H., 2013. β -catenin-driven binary fate specification segregates germ layers in ascidian embryos. *Curr Biol* 23, 491-495.
- Hudson, C., Sirour, C., Yasuo, H., 2016. Co-expression of *Foxa.a*, *Foxd* and *Fgf9/16/20* defines a transient mesendoderm regulatory state in ascidian embryos. *Elife* 5, e14692.
- Imai, K., Satoh, N., Satou, Y., 2002a. Early embryonic expression of FGF4/6/9 gene and its role in the induction of mesenchyme and notochord in *Ciona savignyi* embryos. *Development* 129, 1729-1738.
- Imai, K., Takada, N., Satoh, N., Satou, Y., 2000. β -catenin mediates the specification of endoderm cells in ascidian embryos. *Development* 127, 3009-3020.
- Imai, K.S., Hikawa, H., Kobayashi, K., Satou, Y., 2017. *Tfap2* and *Sox1/2/3* cooperatively specify ectodermal fates in ascidian embryos. *Development* 144, 33-37.
- Imai, K.S., Hino, K., Yagi, K., Satoh, N., Satou, Y., 2004. Gene expression profiles of transcription factors and signaling molecules in the ascidian embryo: towards a comprehensive understanding of gene networks. *Development* 131, 4047-4058.
- Imai, K.S., Hudson, C., Oda-Ishii, I., Yasuo, H., Satou, Y., 2016. Antagonism between beta-catenin and *Gata.a* sequentially segregates the germ layers of ascidian embryos. *Development* 143, 4167-4172.
- Imai, K.S., Levine, M., Satoh, N., Satou, Y., 2006. Regulatory blueprint for a chordate embryo. *Science* 312, 1183-1187.
- Imai, K.S., Satoh, N., Satou, Y., 2002b. An essential role of a *FoxD* gene in notochord induction in *Ciona*

- embryos. *Development* 129, 3441-3453.
- Kawai, N., Iida, Y., Kumano, G., Nishida, H., 2007. Nuclear accumulation of beta-catenin and transcription of downstream genes are regulated by zygotic Wnt5alpha and maternal Dsh in ascidian embryos. *Dev Dyn* 236, 1570-1582.
- Kimelman, D., Kirschner, M., Scherson, T., 1987. The Events of the Midblastula Transition in *Xenopus* Are Regulated by Changes in the Cell-Cycle. *Cell* 48, 399-407.
- Kobayakawa, Y., Kubota, H.Y., 1981. Temporal Pattern of Cleavage and the Onset of Gastrulation in Amphibian Embryos Developed from Eggs with the Reduced Cytoplasm. *J Embryol Exp Morph* 62, 83-94.
- Kumano, G., Nishida, H., 2009. Patterning of an ascidian embryo along the anterior-posterior axis through spatial regulation of competence and induction ability by maternally localized PEM. *Dev Biol* 331, 78-88.
- Kumano, G., Takatori, N., Negishi, T., Takada, T., Nishida, H., 2011. A maternal factor unique to ascidians silences the germline via binding to P-TEFb and RNAP II regulation. *Curr Biol* 21, 1308-1313.
- Langley, A.R., Smith, J.C., Stemple, D.L., Harvey, S.A., 2014. New insights into the maternal to zygotic transition. *Development* 141, 3834-3841.
- Lu, X.M., Li, J.M., Elemento, O., Tavazoie, S., Wieschaus, E.F., 2009. Coupling of zygotic transcription to mitotic control at the *Drosophila* mid-blastula transition. *Development* 136, 2101-2110.
- Matsuoka, T., Ikeda, T., Fujimaki, K., Satou, Y., 2013. Transcriptome dynamics in early embryos of the ascidian, *Ciona intestinalis*. *Dev Biol* 384, 375-385.
- Miya, T., Nishida, H., 2003. Expression pattern and transcriptional control of SoxB1 in embryos of the ascidian *Halocynthia roretzi*. *Zool Sci* 20, 59-67.
- Negishi, T., Takada, T., Kawai, N., Nishida, H., 2007. Localized PEM mRNA and protein are involved in cleavage-plane orientation and unequal cell divisions in ascidians. *Curr Biol* 17, 1014-1025.
- Newport, J., Kirschner, M., 1982a. A Major Developmental Transition in Early *Xenopus*-Embryos .I. Characterization and Timing of Cellular-Changes at the Midblastula Stage. *Cell* 30, 675-686.
- Newport, J., Kirschner, M., 1982b. A major developmental transition in early *Xenopus* embryos: II. Control of the onset of transcription. *Cell* 30, 687-696.
- Nishida, H., Sawada, K., 2001. macho-1 encodes a localized mRNA in ascidian eggs that specifies muscle fate during embryogenesis. *Nature* 409, 724-729.
- Nishikata, T., Yamada, L., Mochizuki, Y., Satou, Y., Shin-i, T., Kohara, Y., Satoh, N., 2001. Profiles of maternally expressed genes in fertilized eggs of *Ciona intestinalis*. *Dev Biol* 238, 315-331.
- Oda-Ishii, I., Kubo, A., Kari, W., Suzuki, N., Rothbacher, U., Satou, Y., 2016. A Maternal System Initiating the Zygotic Developmental Program through Combinatorial Repression in the Ascidian Embryo. *PLoS genetics* 12, e1006045.

- 424 Ogura, Y., Sakaue-Sawano, A., Nakagawa, M., Satoh, N., Miyawaki, A., Sasakura, Y., 2011. Coordination of
- 425 mitosis and morphogenesis: role of a prolonged G2 phase during chordate neurulation. *Development* 138,
- 426 577-587.
- 427 Ogura, Y., Sasakura, Y., 2016. Developmental Control of Cell-Cycle Compensation Provides a Switch for
- 428 Patterned Mitosis at the Onset of Chordate Neurulation. *Dev Cell* 37, 148-161.
- 429 Ohta, N., Satou, Y., 2013. Multiple signaling pathways coordinate to induce a threshold response in a chordate
- 430 embryo. *PLoS genetics* 9, e1003818.
- 431 Ohta, N., Waki, K., Mochizuki, A., Satou, Y., 2015. A Boolean Function for Neural Induction Reveals a
- 432 Critical Role of Direct Intercellular Interactions in Patterning the Ectoderm of the Ascidian Embryo. *PLoS*
- 433 *Comput Biol* 11, e1004687.
- 434 Rothbächer, U., Bertrand, V., Lamy, C., Lemaire, P., 2007. A combinatorial code of maternal GATA, Ets and
- 435 β -catenin-TCF transcription factors specifies and patterns the early ascidian ectoderm. *Development* 134,
- 436 4023-4032.
- 437 Satou, Y., Imai, K.S., 2015. Gene regulatory systems that control gene expression in the *Ciona* embryo. *Proc*
- 438 *Jpn Acad Ser B Phys Biol Sci* 91, 33-51.
- 439 Satou, Y., Kawashima, T., Shoguchi, E., Nakayama, A., Satoh, N., 2005. An integrated database of the
- 440 ascidian, *Ciona intestinalis*: Towards functional genomics. *Zool Sci* 22, 837-843.
- 441 Satou, Y., Kusakabe, T., Araki, S., Satoh, N., 1995. Timing of Initiation of Muscle-Specific Gene-Expression
- 442 in the Ascidian Embryo Precedes That of Developmental Fate Restriction in Lineage Cells. *Dev Growth*
- 443 *Differ* 37, 319-327.
- 444 Satou, Y., Mineta, K., Ogasawara, M., Sasakura, Y., Shoguchi, E., Ueno, K., Yamada, L., Matsumoto, J.,
- 445 Wasserscheid, J., Dewar, K., Wiley, G.B., Macmil, S.L., Roe, B.A., Zeller, R.W., Hastings, K.E.M., Lemaire,
- 446 P., Lindquist, E., Endo, T., Hotta, K., Inaba, K., 2008. Improved genome assembly and evidence-based global
- 447 gene model set for the chordate *Ciona intestinalis*: new insight into intron and operon populations. *Genome*
- 448 *Biol* 9, R152.
- 449 Satou, Y., Yagi, K., Imai, K.S., Yamada, L., Nishida, H., Satoh, N., 2002. *macho-1*-Related genes in *Ciona*
- 450 embryos. *Dev Genes Evol* 212, 87-92.
- 451 Shimauchi, Y., Chiba, S., Satoh, N., 2001. Synergistic action of HNF-3 and Brachyury in the notochord
- 452 differentiation of ascidian embryos. *Int J Dev Biol* 45, 643-652.
- 453 Shirae-Kurabayashi, M., Matsuda, K., Nakamura, A., 2011. Ci-Pem-1 localizes to the nucleus and represses
- 454 somatic gene transcription in the germline of *Ciona intestinalis* embryos. *Development* 138, 2871-2881.
- 455 Tadros, W., Lipshitz, H.D., 2009. The maternal-to-zygotic transition: a play in two acts. *Development* 136,
- 456 3033-3042.

457 Takatori, N., Hotta, K., Mochizuki, Y., Satoh, G., Mitani, Y., Satoh, N., Satou, Y., Takahashi, H., 2004. T-box
458 genes in the ascidian *Ciona intestinalis*: Characterization of cDNAs and spatial expression. *Dev Dyn* 230,
459 743-753.

460 Wada, S., Hamada, M., Kobayashi, K., Satoh, N., 2008. Novel genes involved in canonical Wnt/beta-catenin
461 signaling pathway in early *Ciona intestinalis* embryos. *Dev Growth Differ* 50, 215-227.

462 Yoshida, S., Marikawa, Y., Satoh, N., 1996. Posterior end mark, a novel maternal gene encoding a localized
463 factor in the ascidian embryo. *Development* 122, 2005-2012.

464

465

Figure Legends

Figure 1. Analysis of the onset of zygotic gene expression by *in situ* hybridization. Expression of (A) *Foxa.a*, (B) *Sox1/2/3*, (C) *Efna.d*, (D) *Tfap2-r.b*, (E) *Foxd*, (F) *Fgf9/16/20*, and (G) *Tbx6.b* at the 2- to 16-cell stages revealed by *in situ* hybridization. Arrowheads indicate expression. Ant, anterior side; pos, posterior side; ani, animal side; veg, vegetal side. Scale bar, 100 μ m.

Figure 2. Analysis of the onset of zygotic gene expression by RT-qPCR. Temporal gene expression profiles of (A) *Foxa.a*, (B) *Sox1/2/3*, (C) *Efna.d*, (D) *Tfap2-r.b*, (E) *Foxd*, (F) *Fgf9/16/20*, (G) *Tbx6.b*, and (H) *Gata.a* revealed by RT-qPCR and shown as relative values against expression levels at the 16-cell stage. Maternal *Zic-r.a* mRNA was used as the endogenous control. Three independent experiments were performed and are represented by differently colored bars. Differences in expression levels between the 2- and 4-cell stages and between the 4- and 8-cell stages were analyzed by paired t-test. Significant differences (less than 5%) are shown in panels. Note that *Gata.a* is maternally expressed and included as a control.

Figure 3. Expression of a *Gfp* reporter construct containing the upstream region of *Efna.d* in early embryos. (A) The ratio of embryos that expressed *Gfp* mRNA at the 2-cell and 16-cell stages was revealed by *in situ* hybridization. Two independent experiments were performed and are represented by differently colored bars. (B) Temporal expression profiles of the reporter genes were measured by RT-qPCR and shown as relative values against expression levels at the 16-cell stage. Maternal *Zic-r.a* mRNA was used for normalizing the data. Two independent experiments were performed and are represented by differently colored bars.

Figure 4. Expression of *Efna.d* in the animal and vegetal hemispheres at the 8-cell stage. (A)

Expression of the reporter gene, containing the upstream region of *Efna.d*, at the 8-stage, was revealed by *in situ* hybridization. Weak signals can be observed in the vegetal cells (A4.1 and B4.1) and strong signals in the animal cells (a4.2 and b4.2) of 8-cell embryos. Scale bar, 100 μ m. (B) The ratio of embryos that expressed *Gfp* mRNA at the 8-cell stage. We regarded clear spots [which were similar to the spots in the animal cells of the 8-cell embryos shown in (A)] as strong, and faint spots [which were similar to the spots in the vegetal cells of the 8-cell embryos shown in (A)] as weak. We examined 58 embryos from two batches. (C) The amount of endogenous *Efna.d* mRNA in unfertilized eggs, fertilized eggs, 2-, 4-, 8-, and 16-cell embryos was measured using RT-qPCR with a set of intron primers that amplify a sequence within the first intron. *Pou2* was used for normalizing the data. Three independent experiments were performed and are represented by differently colored bars. No specific amplification was detected in early embryos (nd). (D) Methodology for the experiment to examine the expression of endogenous *Efna.d* in the animal and vegetal halves of 8-cell embryos. At the 8-cell stage, the animal and vegetal hemispheres were isolated using a fine glass needle. (E) The amount of endogenous *Efna.d* mRNA in the animal and vegetal hemispheres was measured using RT-qPCR. *Pou2* was used for normalizing the data. Two independent experiments were performed and are represented by differently colored bars. Amplification was not detected in negative control samples in which reverse transcriptase was not added (nd).

Figure 5. Expression and distribution of Gata.a and β -catenin. (A) Immunostaining of early embryos with antibodies against Gata.a. All nuclei are stained. In the bottom panels, nuclei are shown by DAPI staining. Images are Z-projected image stacks. Scale bar, 100 μ m. (B) A western blot using the antibodies against Gata.a. Lysates prepared from 200 embryos were loaded in each lane. In two independent

experiments, the bands were quantified, and the intensities are shown as relative values to those of embryos at the 16-cell stage. Results of the two experiments are shown using different colors. (C) Immunostaining of early embryos with antibodies against β -catenin. In the bottom panels, nuclei are shown by DAPI staining. Images are Z-projected image stacks. The brightness and contrast levels were linearly adjusted. Note that nuclei, except for those in the vegetal cells, of 16-cell embryos lack signals. Scale bar, 100 μ m. (D) Quantification of fluorescence intensities of signals for nuclear and cytoplasmic β -catenin. The y-axis represents nuclear/cytoplasmic ratios for β -catenin signal intensity. Difference between the animal and vegetal halves of 8-cell and 16-cell embryos was tested by the Wilcoxon rank sum test. All data measured are plotted as individual dots and summarized values are shown as box-and-whisker plots.

Figure 6. Expression of *Foxa.a*, *Efna.d*, and *Foxd* in *Pem-1* morphants. In *Pem-1* morphants, (A) signals for *Foxa.a* expression were observed in all blastomeres at the 8-cell stage, while no signals for (B) *Efna.d* and (C) *Foxd* expression were observed. The number of embryos examined and percentage of embryos that expressed *Foxa.a*, *Efna.d*, and *Foxd* are shown in each photograph. Lateral views are shown. Note that *Pem-1* morphants show defects in the anterior–posterior axis (Negishi et al., 2007). Arrowheads indicate expression. Scale bar, 100 μ m.

Figure 7. Nuclear translocation of β -catenin and *Foxd* expression in embryos treated with the GSK3 inhibitor BIO. (A, B) Immunostaining of BIO-treated embryos with antibodies against β -catenin. (A', B') DAPI staining indicates the nuclei of the embryos shown in (A) and (B). Images are Z-projected image stacks. (C) Quantification of fluorescence intensities of signals for nuclear and cytoplasmic β -catenin in BIO-treated embryos. The y-axis represents nuclear/cytoplasmic ratios of β -catenin signal

intensity. All data measured are plotted as individual dots and summarized values are shown as box-and-whisker plots. (D) The relative *Foxd* expression level in BIO-treated embryos and DMSO-treated control embryos was measured using RT-qPCR. Three independent experiments were performed, and are represented by differently colored bars. Paired *t*-tests were performed for comparing data between the 4- and 8-cell embryos treated with BIO and between the 8-cell embryos with and without the BIO treatment, and showed significant differences. (E) *In situ* hybridization of *Foxd* in an 8-cell embryo treated with BIO. Arrowheads indicate *Foxd* expression.

Figure 8. Expression of *Foxd* initiates at the 8-cell stage in *Cdc25* morphants. (A, B) Injection of a MO against the cell-cycle regulator *Cdc25* extends the lengths of the cell-cycle. (A) Averaged cell cycle lengths are shown in bars. (B) The average time duration of cell divisions for wild type embryos, embryos injected with a control *lacZ* MO, and embryos injected with the *Cdc25* MO. (C, D) Expression of *Foxd* in *Cdc25* morphants at the (C) 4-cell and (D) 8-cell stages. The number of embryos examined and proportion of embryos that expressed *Foxd* are shown within the panels. Arrowheads indicate expression. Scale bar, 100 μ m. (E) The amount of *Foxd* mRNA was measured using RT-qPCR at 130 min after fertilization in embryos injected with *lacZ* (control) MO or *Cdc25* MO. Three independent experiments were performed and are represented by differently colored bars.

546 **Table 1. Names and identifiers for genes that were used in the present study**

Gene name	Gene identifier
<i>Foxd</i>	CG.KH2012.C8.396/890
<i>Sox1/2/3</i>	CG.KH2012.C1.99
<i>Efna.d</i>	CG.KH2012.C3.716
<i>Tfap2-r.b</i>	CG.KH2012.C7.43
<i>Fgf9/16/20</i>	CG.KH2012.C2.125
<i>Tbx6.b</i>	CG.KH2012.S6541/2/3
<i>Gata.a</i>	CG.KH2012.L20.1
<i>β-catenin</i>	CG.KH2012.C9.53
<i>Foxa.a</i>	CG.KH2012.C11.313
<i>Pou2</i>	CG.KH2012.C4.85
<i>Zic-r.a (Macho-1)</i>	CG.KH2012.C1.727
<i>Cdc25</i>	CG.KH2012.C5.12

547

548

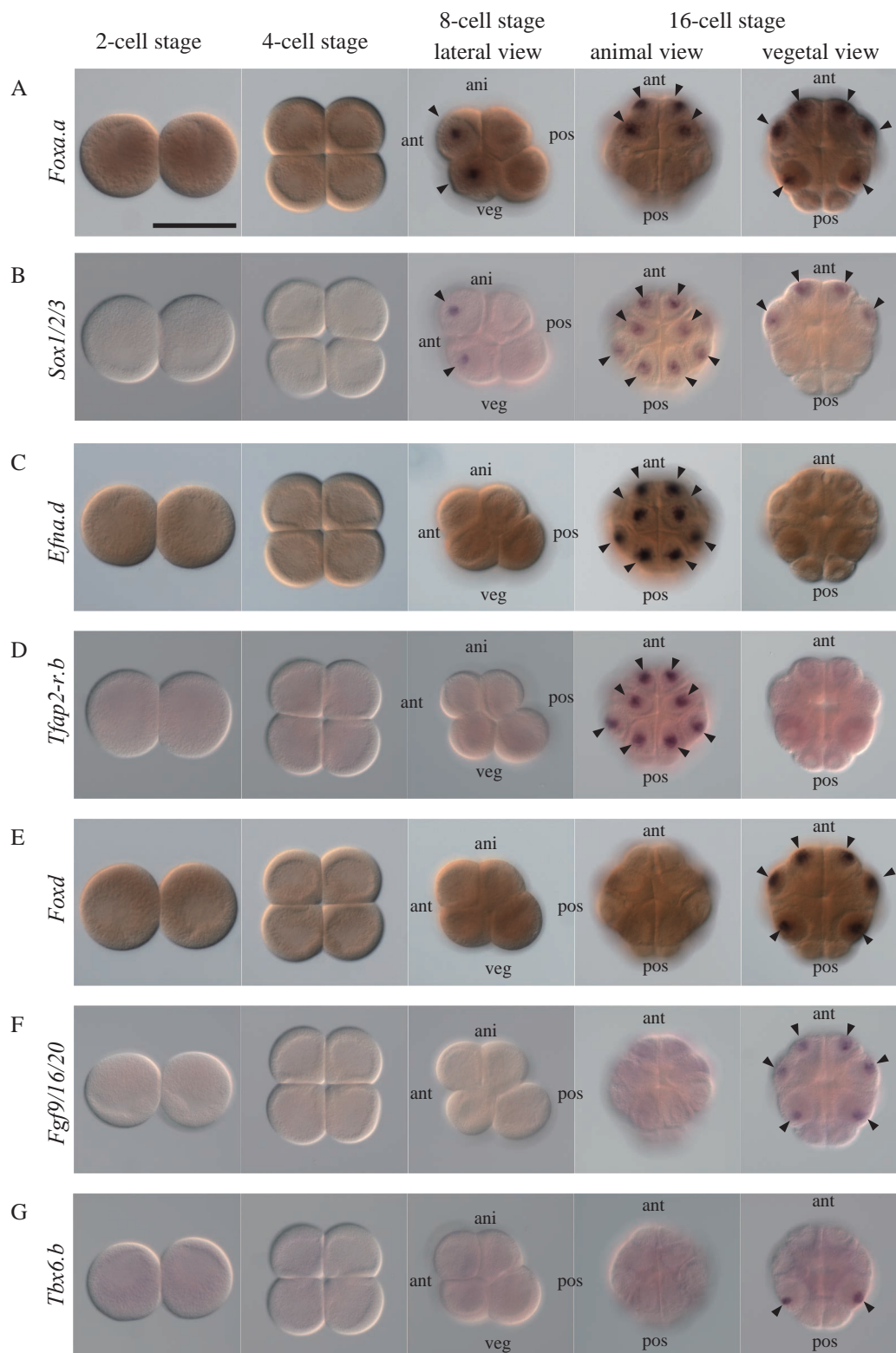
549 **Table 2. Primers and probes used for RT-qPCR.**

Gene	Probes and primers
<i>Foxa.a</i>	Probe : 5'-FAM-TCTGCCGTTGAAGTTAGTTCGCCATCC-TAMRA-3' Forward primer : 5'-TTCAACACCACCACACTCAACAG-3' Reverse primer : 5'-CGTGTTCAATGCCATGTTTC-3'
<i>Sox1/2/3</i>	Probe : 5'-FAM-ATTTATGGTGTGGTCTCGCGGGCAA-TAMRA-3' Forward primer : 5'-CAAAGTACCACAAGAGCAGAGAGTGA-3' Reverse primer : 5'-GGTTGTCCTGTGCCATCTTTCT-3'
<i>Efna.d</i>	Probe : 5'-FAM-TTGTGCTGTACCACGCAACGGAA-TAMRA-3' Forward primer : 5'-CGGATTTCTGTTTCCAGTATTGC-3' Reverse primer : 5'-GCCGCTCTGTTTGCCTCTT-3'
<i>Tfap2-r.b</i>	Probe : 5'-FAM-TACACCAGCTATTTGCGCTGCGATGA-TAMRA-3' Forward primer : 5'-CCAACGACCTCTTACACATTTTCAG-3' Reverse primer : 5'-GATAACGCAGCATCTCCGTTAAGT-3'
<i>Foxd</i>	Probe : 5'-FAM-TCATTATCGTCACCAGCAACCCTTGTACG-TAMRA-3' Forward primer : 5'-AACTCAACATTCAGCTTTGAACGA-3' Reverse primer : 5'-ATTTTCGGCAACCAGTTTTGG-3'
<i>Fgf9/16/20</i>	Probe : 5'-FAM-TTGCCAGGTAGAGACCACTTGCGACACC-TAMRA-3' Forward primer : 5'-ACCCAAGAAAGCCACAATCAATACG-3' Reverse primer : 5'-TCCGAAGCATACAATCTTCCTTTGC-3'
<i>Tbx6.b</i>	Probe : 5'-FAM-CCATTGTTGCCCGCTGCAAGGTGAGT-TAMRA-3' Forward primer : 5'-AACCCCAAGTTCCGCAGAGA-3' Reverse primer : 5'-CATGGAGTGTATGAGGAACCTTTCCA-3'
<i>Gata.a</i>	Probe : 5'-VIC-CCTCAGGACACTTTCTGTGCAGCACG-TAMRA-3' Forward primer : 5'-AACCACGTGAGTGCGTGAAC-3' Reverse primer : 5'-ACAGGTGCCCGCATATAGCTA-3'
<i>Zic-r.a</i>	Probe : 5'-VIC-ACGGTCACTTTTAGCACCTCCACCA-TAMRA-3' Forward primer : 5'-CCCAGTATGCACCAAATTCAGA-3' Reverse primer : 5'-TGGTGAGAAAACGGGTGAAAC-3'
<i>Efna.d</i> intron (Fig. 4)	Forward primer : 5'-TGCCAAGGCCGATTACGA-3' Reverse primer : 5'-CGGGCGGCAGTTTCG-3'
<i>Pou2</i>	Forward primer : 5'-TACCACAGCATACACTGGACAACA-3' Reverse primer : 5'-GGCGCTGAGGTAATGCTTTG-3'
<i>Gfp</i>	Forward primer : 5'-GGGCACAAGCTGGAGTACAAC-3' Reverse primer : 5'-TGGCCTTGATGCCGTTCT-3'

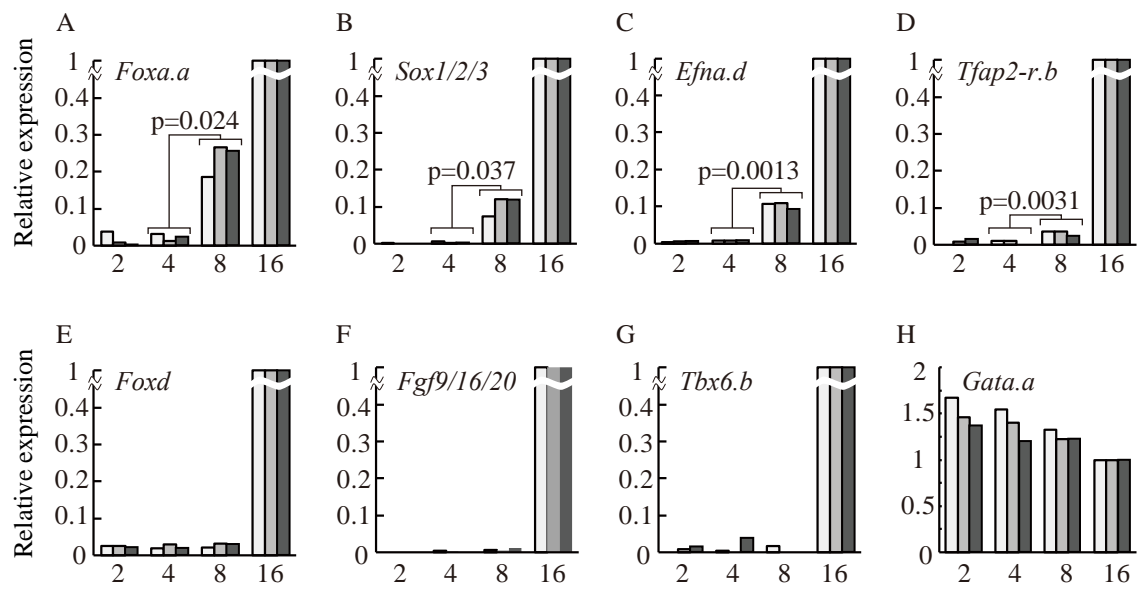
550 Note that the last three sets of primers were used for measurement by the SYBR Green method and no

551 probes were used.

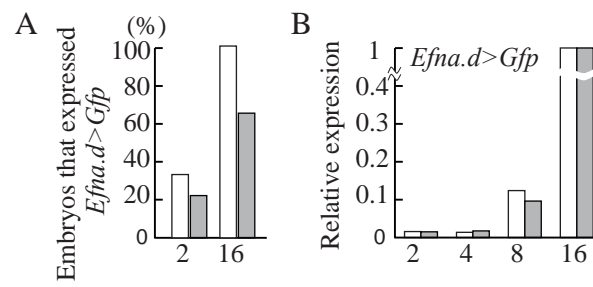
Oda Fig.1



Oda Fig.2



Oda Fig. 3



A

Efna.d>Gfp

a4.2 b4.2
A4.1 B4.1

B

Embryos that expressed *Efna.d>Gfp*

Region	Embryo	Weak (%)	Strong (%)
animal	a4.2	0	100
	b4.2	0	100
vegetal	A4.1	45	10
	B4.1	30	15

C

Stage	Weak (%)	Strong (%)
uFert	nd	nd
Fert	nd	nd
2-cell	0.12	0
4-cell	nd	nd
8-cell	10	10
16-cell	100	100

D

a4.2 b4.2
A4.1 B4.1

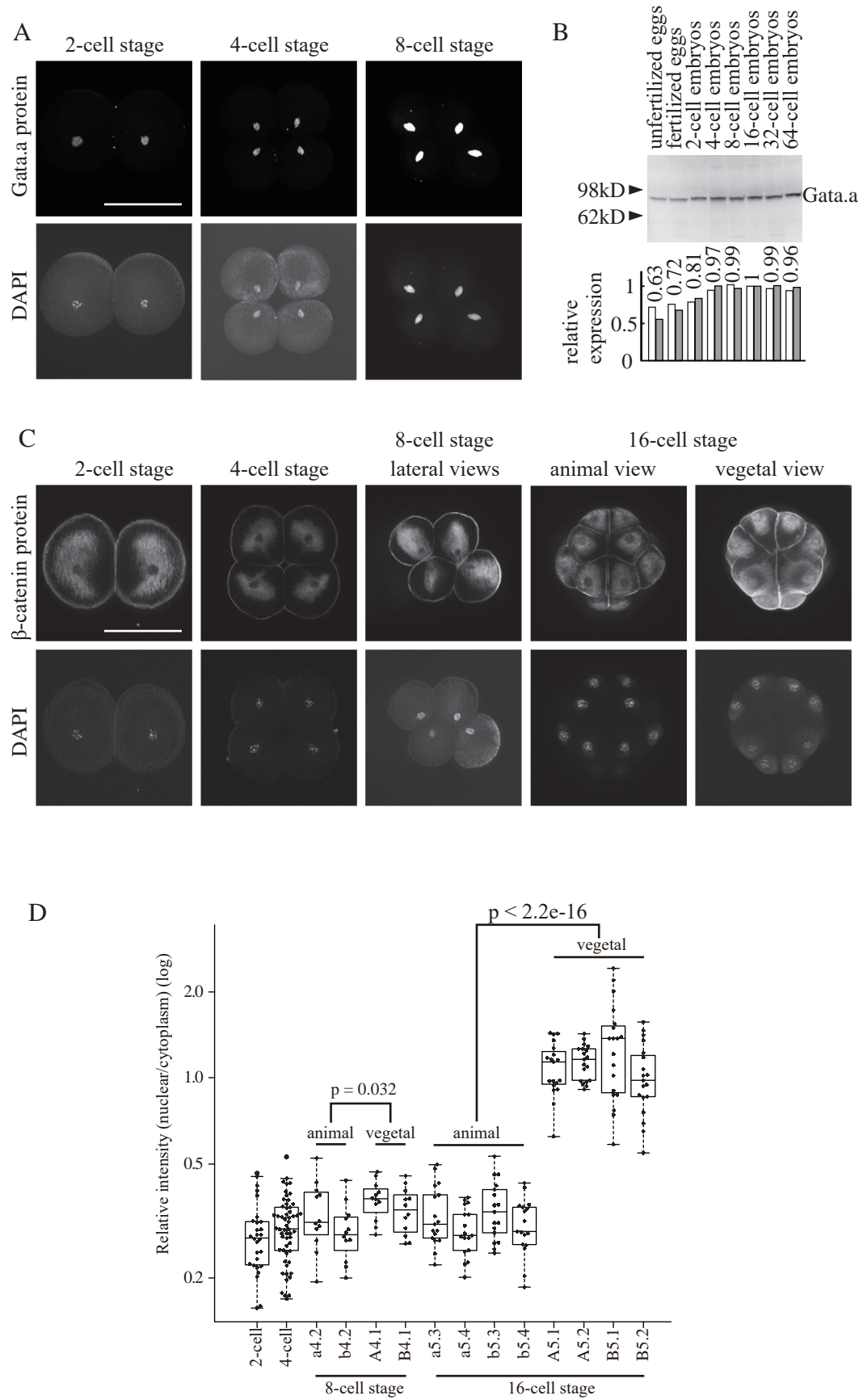
animal half → RT-qPCR
vegetal half → RT-qPCR

E

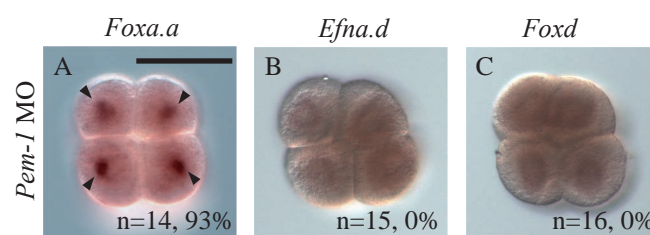
Relative *Efna.d* expression

Condition	Region	Relative Expression
RT+	animal	1.0
	vegetal	1.0
RT-	animal	0.05
	vegetal	0.1
	animal	nd
	vegetal	nd

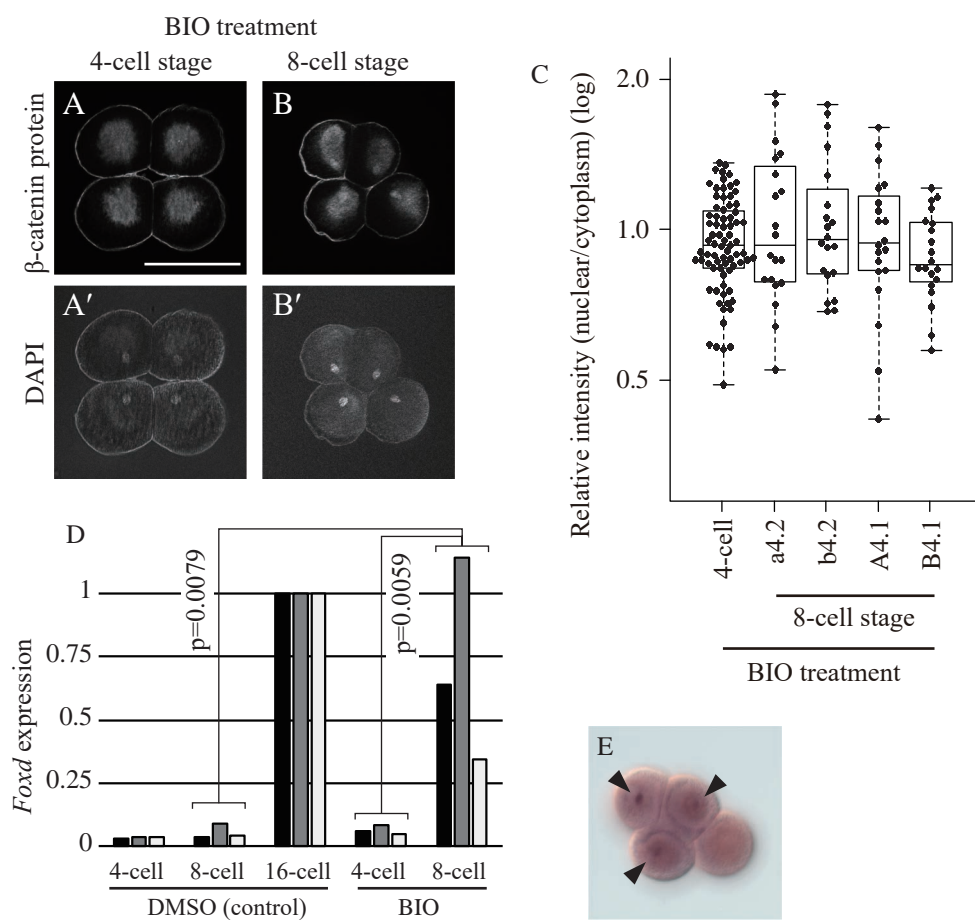
Oda Fig. 5



Oda Fig. 6



Oda Fig. 7



Oda Fig. 8

